# EMI Modelling of an 80 kHz to 80 MHz Wideband Antenna and Low-Noise Amplifier for Radio Astronomy in Space

D.S. Prinsloo[1], M. Ruiter[1], M.J. Arts[1], J. v.d. Marel[1], A.J. Boonstra[1], G. Kruithof[1], M. Wise[1], H. Falcke[2], M. Klein-Wolt[2], H. Rothkaehl[3], B. Cecconi[4], M. Dekkali[4], J. Ping[5]

[1] The Netherlands Institute for Radio Astronomy (ASTRON), Dwingeloo, The Netherlands, prinsloo@astron.nl
[2] Radboud University, Astronomy Department, Nijmegen, The Netherlands
[3] Space Research Centre (SRC) of the Polish Academy of Sciences, Warsaw, Poland
[4] LESIA, Observatoire de Paris, PSL Research University, CNRS, Meudon, France
[5] National Astronomical Observatories of China (NAOC, CAS), Beijing, China

***Abstract*— The methodology followed to model the signals coupled into the analog signal path of the Netherlands-China Low-frequency Explorer due to electromagnetic interference produced by the Chang'e-4 satellite is presented. Results indicate interfering signals at frequencies below 1 MHz pose the highest risk to drive the first stage amplifiers into their non-linear region. This paper subsequently describes mitigation measures to meet this challenge.**

***Index Terms*—omnidirectional antenna, electromagnetic interference, radio astronomy, space technology.**

## I. Introduction

In 2018, the Netherlands-China Low-frequency Explorer (NCLE) [1] will launch on-board the Chang'e-4 satellite [2] to the second Earth-Moon Lagrangian point on the far-side of the Moon. Once in position, NCLE will open the virtually unexplored frequency range below 10 MHz to radio astronomy [3][4]. It will conduct solar and planetary science, determine the radio background spectrum at the Earth-Moon L2 point, and as a precursor to a larger array it will constrain the redshifted 21-cm line Dark Ages and Cosmic Dawn signal.

The instrument comprises three five-meter long monopole antennas each connected to a receiving channel amplifying and sampling signals over the frequency band ranging from 80 kHz to 80 MHz. The system is optimized for 1-30 MHz, but the spectral coverage is extended to higher frequencies for cross-referencing with Earth-based radio telescopes, and to lower frequencies albeit with reduced sensitivity there. Given that the primary function of the Chang'e-4 satellite is to serve as a relay antenna for a lander / rover to be placed on the lunar far side, Electromagnetic Interference (EMI) requirement levels of the satellite are designed to adhere to military standards [5]. These standards, however, were not set up with sensitive radio astronomy receivers in-mind.

This paper therefore presents the design procedure followed to model and mitigate the EMI generated by the satellite. An overview of the NCLE antennas and their electromagnetic performance is given in Sec. II. The technique used to model the interference from the satellite is described in Sec. III. Lastly, the architecture of the low-noise amplifier (LNA) design implemented in the NCLE instrument to mitigate the EMI generated by the spacecraft is presented in Sec. IV.

## II. NCLE Antennas

Figure 1 shows the simplified model of the Chang'e-4 satellite used to simulate the performance of the NCLE antennas. As indicated, three five-meter long antennas will be co-located on a single panel behind the relay reflector antenna.

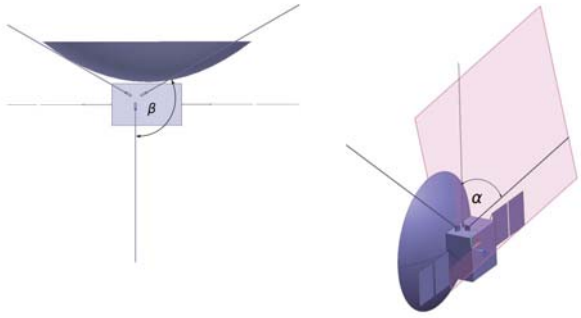


(a) (b)

Fig. 1. Simulated model of the NCLE antennas (a) top view, and (b) perspective view indicating the in-plane antenna separation angle α.

Each of the three antennas extend outward at an angle of 45° with respect to the spacecraft panel to which the they are connected. As shown in Fig. 1(a) the projected angle between antennas, β, is 120°. Considering a plane intersecting any pair of antennas [c.f. Fig. 1(b)], two antennas are separated by an angle, α, equal to 75.5°.

The decision to implement five-meter monopole antennas follows from a previous study performed for a similar space-based low-frequency telescope concept [6]. Using the sky noise temperature as a reference, the required LNA noise

temperature for various antenna lengths is compared to ensure a sky noise limited system.

The study in [6] shows that antenna lengths of one- or two-meter require LNAs with a noise temperature below 50 K at frequencies below 1 MHz. In comparison five-meter antennas are sky noise limited for LNAs with noise temperatures around 100 K – a design requirement that is easier to realize. Although the LNA noise temperature requirement becomes less stringent for antennas that are longer than five meters, the lower resonant frequency makes longer antennas a less attractive option for NCLE.

### *A. Radiation Performance*

At five-meter length, each antenna is resonant around 15 MHz. Figure 2 shows the simulated radiation patterns of the three monopole antennas at 9 MHz.

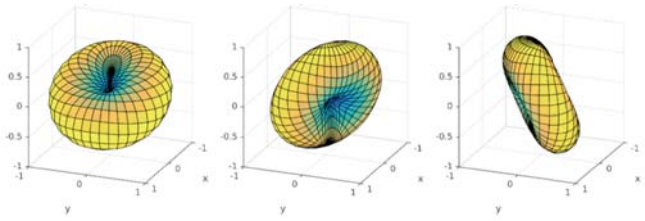

Fig. 2. NCLE monopole element patterns at 9 MHz.

As seen, the spacecraft has little effect on the radiation performance of the NCLE antennas at frequencies below the first resonant frequency: the direction of maximum directivity remains approximately normal to the orientation of each antenna. For frequencies above 15 MHz, the spacecraft has a much larger effect on the radiation of each antenna. This effect is clearly seen in the polarimetric performance of the NCLE antennas detailed in the following section.

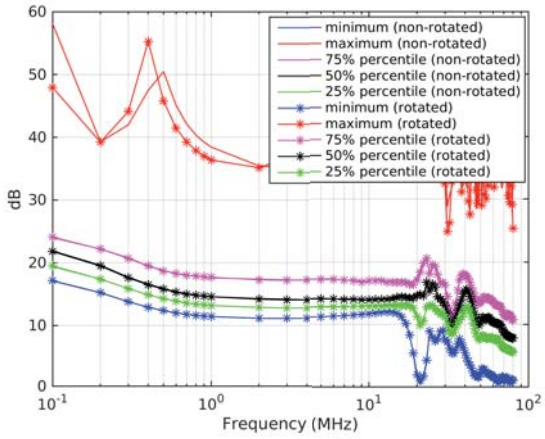


Fig. 3. Intrinsic cross-polarization ratio percentiles of the NCLE antennas over frequency.

### *B. Polarimetric Performance*

To assess the polarimetric performance of the NCLE antenna system, the Intrinsic Cross polarization Ratio (IXR) [7] is used. The graph in Fig. 3 shows the minimum and maximum IXR values, together with the 25, 50, and 75 percentile values over a full spherical field-of-view (FoV) coverage achieved with the three monopole antennas from 100 kHz up to 80 MHz. For each percentile value two curves are shown: one with the solar panels positioned as indicated in Fig. 1 (non-rotated) and another for which the solar panels are rotated by 90° (rotated).

Firstly, it is clear from Fig. 3 that the orientation of the solar panels has little effect on the polarimetric performance of the NLCE antennas. Furthermore, the spacecraft's influence on the radiation patterns of the antennas becomes apparent at frequencies above the first resonant frequency where, above 15 MHz, the IXR values are seen to vary rapidly over frequency. Despite this variation the 50% percentile of the IXR remains above 10 dB over most of the operating frequency band.

## III. SPACECRAFT EMI

The location of the NCLE antennas on the spacecraft influence not only the radiation performance of the antennas, as discussed in Sec. II, but also make the NCLE instrument susceptible to interference produced by the spacecraft. Since initially no EMI measurements were available for the Chang'e-4 satellite, the following strategy has been followed to obtain a worst-case value for the interference levels from the spacecraft.

### *A. Conducted Emmisions*

Electromagnetic interference from the Chang'e-4 satellite must adhere to the specifications stated in MIL-STD-461 [2]. In this analysis one of the predominant interference sources has been identified as the power leads connecting the solar panels to the interior of the satellite, i.e. current induced on these power leads can couple into the NLCE front-end through the three NCLE antennas.

MIL-STD-461 requirement CE102 specify the maximum conducted emissions on power leads from 10 kHz to 10 MHz. Given that the NCLE frequency band extends to 80 MHz, the conducted emissions from 10 MHz to 80 MHz are assumed constant in this analysis.

### *B. EMI Modelling*

Figure 4 shows the equivalent spacecraft model simulated in Wipl-D. In the simulation, ports 1 to 3 excite the monopole antennas and ports 4 to 7 connect the sides of the spacecraft to the solar panel power leads. Through solving the seven-port scattering matrix, the voltage induced at each antenna port due to current induced on the solar panel power leads can be determined as outlined below.

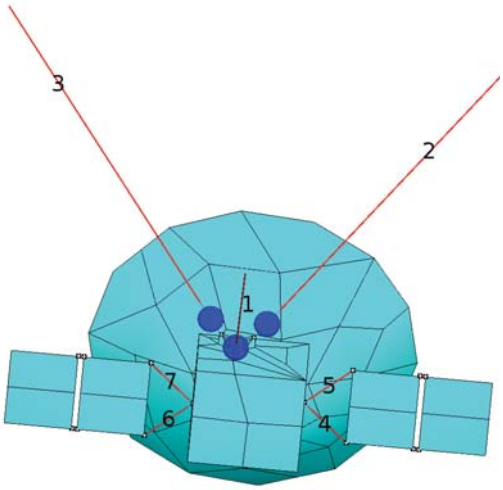


Fig. 4. Equivalent spacecraft model used to solve the EMI coupled into the NCLE antennas due to conducted emmissions on power leads of the solar panels.

First, consider the schematic representation of each of the current sources positioned at ports 4 to 7 as shown in Fig. 5(a). For a real source impedance ($Z_0$) the incident power wave ($a$) can be expressed in terms of current ($J$), i.e.

$$a = \frac{1}{2} J \sqrt{Z_0} \tag{1}$$

Considering the schematic representation of each terminated antenna port shown in Fig. 5(b), the power wave reflected from each antenna port ($b$) can be expressed in terms of port voltage ($V$)

$$b = \sqrt{Re\{Z_L\}} \frac{V}{Z_L} \tag{2}$$

with $Z_L$ denoting the load impedance in which each antenna is terminated. Using the coupling between a port ($p$) on the solar panel power leads and one of the antenna ports ($q$) – $S_{qp}$ – the power reflected from an antenna port ($b_q$) due to an incident wave on the solar panel power leads ($a_p$) can be solved, i.e.

$$b_q = S_{qp} a_p \tag{3}$$

Or, substituting (1) and (2) in (3), the voltage across a load on antenna port $q$ – $V_q$ – can be expressed in terms of the current induced on the solar panel power lead positioned at port $p$ – $J_p$ – where,

$$V_q = S_{qp} \frac{\sqrt{Z_0}\, Z_L}{2\sqrt{Re\{Z_L\}}} J_p \tag{4}$$

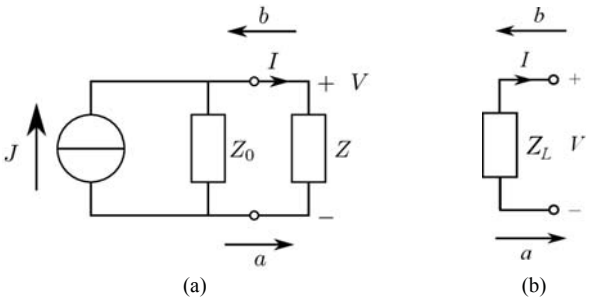


Fig. 5. Schematic representations of (a) the equivalent current sources connected to the solar panel power leads, and (b) the load in which each NCLE antenna is terminated.

Following from (4), the worst-case open circuit spectral voltage density induced at the antenna ports is solved for spectral current densities defined according to the CE102 requirements of MIL-STD-461. Note that, in solving (4), the simulated scattering matrix must be transformed to the appropriate port impedances, i.e. numerically infinite for both the current sources and the open circuit loads at the antenna ports. Figure 6 shows the simulated open circuit spectral voltage density induced at the antenna ports due to conducted emissions solved using the procedure described in this section.

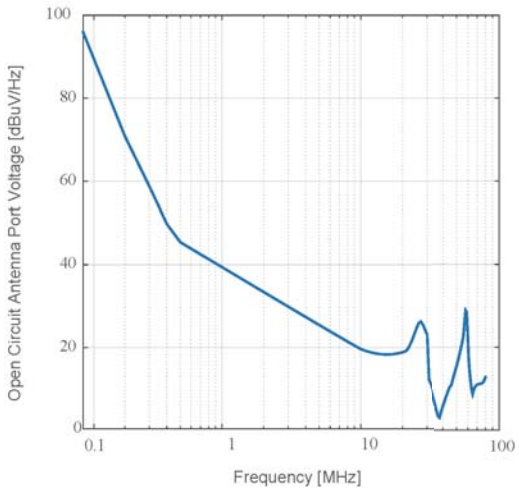


Fig. 6. Maximum simulated open circuit voltage at the NCLE antenna ports due to spurious currents induced on the solar panel power leads.

## IV. LNA Architecture

Given the anticipated EMI levels depicted in Fig. 6, it is clear that EMI signals induced at frequencies below 1 MHz pose a high risk of driving the active components in the analog signal path into their non-linear operating region. To mitigate this risk, each analog channel on the LNA is designed to select between three frequency bands – limiting the instantaneous power at the input of the first amplification

stage. A simplified block diagram of one analog channel on the LNA-board is shown in Fig. 7.

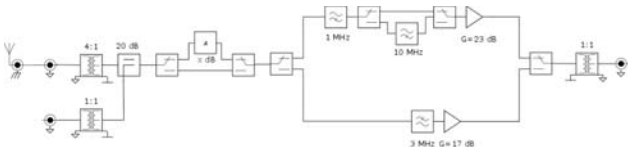


Fig. 7. Block diagram of a single channel on the NCLE LNA-board.

On the LNA-board, each analog channel has two input ports: one interfaced with one of the monopole antennas and another allowing for a calibration signal to be coupled into the analog signal path through a 20 dB directional coupler. Transformers are used at all ports to isolate the LNA from the spacecraft chassis. At the antenna input port, a transformer with at 4:1 turn ratio is implemented to reduce the magnitude of EMI signals produced by the spacecraft.

The analog signal path is further divided into two distinct paths: a low-band comprising a 3 MHz low-pass filter and a high-band consisting of a 1 MHz high-pass filter. Since the largest EMI signals are expected at frequencies below 1 MHz [c.f. Fig. 6], a highly linear operational amplifier (THS4511 from Texas Instruments) is implemented in the low-band. For the high-band, a large portion of EMI from the spacecraft is filtered by the 1 MHz high-pass filter and therefore an operational amplifier with larger gain (AD8001 from Analog Devices) is used in the high-band. In addition to the 1 MHz filter, a 10 MHz high-pass filter can be selected within the high-band to further reduce the EMI levels when observing at these frequencies. As a last resort, each channel has the functionality to switch to a fixed attenuation prior to the band selection thereby ensuring the amplifiers operate within their linear region, albeit at the expense of added system noise.

## V. CONCLUSION

This paper provides an overview of the NCLE antenna and LNA system to be placed on the Chang'e-4 relay satellite. The procedure followed to simulate the voltage levels induced at the antenna ports due to spurious currents on the solar panel power leads is described. Using this procedure, the maximum open circuit voltage at the antenna ports is solved for the conducted emissions limits specified in MIL-STD-461. The results show that the interference levels at frequencies below 1 MHz pose the largest risk to drive the first stage amplifiers into saturation. Lastly, the LNA architecture implemented to mitigate this risk is discussed. In future work, the sensitivity of the NCLE antenna and LNA system will be presented.

## ACKNOWLEDGMENT

NCLE is funded through ESA PRODEX and the Netherlands Space Office (NSO). Thanks to our partners TUDelft, UT, TuE, JIVE ERIC, and IRF for their support.

## REFERENCES

[1] A.J. Boonstra *et al.*, "The Netherlands – China Low Frequency Explorer," 32nd International Union of Radio Science (URSI) General Assembly Scientific Symposium (GASS), Montreal, Canada, Aug. 2017, unpublished.

[2] Wu Weiren, Tang Yuhua, Zhang Lihua and Qiao Dong, "Design of communication relay mission for supporting lunar-farside soft landing", Science China Press, Sci. China Inf. Sci., 60(1), 2017

[3] S. Jester and H. Falcke. "Science with a lunar low-frequency array: from the dark ages of the universe to nearby exoplanets," New Astronomy Reviews, 53, pp. 1–26, February 2009

[4] P. Zarka et al., "Planetary and exoplanetary low frequency radio observations from the Moon", Planetary and Space Science 74, pp. 156–166, 2012

[5] *Requirements for the control of electromagnetic interference characteristics of subsystems and equipment*, MIL-STD-461E, 20 August 1999.

[6] M. J. Arts, E. van der Wal and A. J. Boonstra, "Antenna concepts for a space-based low-frequency radio telescope," ESA Antenna Workshop on Antennas for Space Applications, Noordwijk, pp. 5-8, 2010

[7] T.D. Carozzi and G. Woan, "A fundamental figure of merit for radio polarimeters," IEEE Trans. Antennas Propag., vol. 59, no. 6, pp. 2058-2065, June 2011.